



Originally published as:

Kleyböcker, A., Liebrich, M., Kasina, M., Kraume, M., Wittmaier, M., Würdemann, H. (2012): Comparison of different procedures to stabilize biogas formation after process failure in a thermophilic waste digestion system: Influence of aggregate formation on process stability. - Waste Management, 32, 6, 1122-1130

DOI: [10.1016/j.wasman.2012.01.015](https://doi.org/10.1016/j.wasman.2012.01.015)

# **Comparison of different procedures to stabilize biogas formation after process failure in a thermophilic waste digestion system: Influence of aggregate formation on process stability**

A. Kleyböcker, M. Liebrich, M. Kasina, H. Würdemann  
Microbial GeoEngineering, Helmholtz Centre Potsdam, GFZ German Research Centre for Geosciences, 14473  
Potsdam, Germany

M. Kraume  
Chemical & Process Engineering, Technical University Berlin, 10623 Berlin, Germany

M. Wittmaier  
Institute for Recycling and Environmental Protection, Bremen University of Applied Sciences, 28199 Bremen,  
Germany

\*Corresponding author:  
Email: wuerdemann@gfz-potsdam.de  
Phone: (0049)331 288 1516  
Fax: (0049)331 288 1450

## **ABSTRACT**

Following a process failure in a full-scale biogas reactor, different counter measures were undertaken to stabilize the process of biogas formation, including the reduction of the organic loading rate, the addition of sodium hydroxide (NaOH), and the introduction of calcium oxide (CaO). Corresponding to the results of the process recovery in the full-scale digester, laboratory experiments showed that CaO was more capable of stabilizing the process than NaOH. While both additives were able to raise the pH to a neutral milieu ( $\text{pH} > 7.0$ ), the formation of aggregates was observed particularly when CaO was used as the additive. Scanning electron microscopy investigations revealed calcium phosphate compounds in the core of the aggregates. Phosphate seemed to be released by phosphorus-accumulating organisms, when volatile fatty acids accumulated. The calcium, which was charged by the CaO addition, formed insoluble salts with long chain fatty acids, and caused the precipitation of calcium phosphate compounds. These aggregates were surrounded by a white layer of carbon rich organic matter, probably consisting of volatile fatty acids. Thus, during the process recovery with CaO, the decrease in the amount of accumulated acids in the liquid phase was likely enabled by (1) the formation of insoluble calcium salts with long chain fatty acids, (2) the adsorption of volatile fatty acids by the precipitates, (3) the acid uptake by phosphorus-accumulating organisms and (4) the degradation of volatile fatty acids in the aggregates. Furthermore, this mechanism enabled a stable process performance after re-activation of biogas production. In contrast, during the counter measure with NaOH aggregate formation was only minor resulting in a rapid process failure subsequent the increase of the organic loading rate.

## 1. Introduction

The profitability of biogas plants decreases drastically during process failure, followed by a long-term re-establishment of a stable biogas production (Balussou et al. 2011). Furthermore, emissions of methane increase during failure, as the substrate is not digested completely, and the fermented sludge is used by farmers as fertilizer. In order to increase the flexibility of the plant and thus to use different organic substrates and varying loading rates, process understanding has to be improved, and counter measures against process failure have to be developed.

During the process of biogas formation, complex organic matter is converted into methane and carbon dioxide. The process involves hydrolyses, acidogenesis, acetogenesis, and methanogenesis. The first three phases are carried out by hydrolytic and fermentative bacteria, while the methanogenesis is performed by archaea (Schink 1994). Process failures can be caused by different inhibitors such as sulfides, ammonia, heavy metals, phenolic compounds and other toxic substances (Pender et al. 2004, Braun et al. 1981, Karakashev et al. 2005, Veeresh et al. 2005). These substances inhibit the methanogens if their concentration exceeds a critical value. By overloading the digester with organic matter, the methanogens are also inhibited due to an accumulation of long chain fatty acids (LCFAs) (Angelidaki et al. 1992, Rinzema et al. 1993, Hwu et al. 1998, Miron et al. 2000, Kuang et al. 2006, Luostarinen et al. 2009). In the biogas producing microbial community methanogenic archaea are more sensitive to disturbances than several species of the bacteria. Their proceeding metabolism leads to an accumulation of acetic acid and hydrogen, because its consumption by the methanogens is reduced. If the interspecies hydrogen transfer between propionic acid degrading bacteria and methanogens is disturbed, the hydrogen partial pressure exceeds the limit of the thermodynamic window of 0.002 mbar and 0.1 mbar. In consequence, the degradation of propionic acid is inhibited and leads to its accumulation (Aivasidis et al. 2005, Harper et al. 1986). The concentration of other VFAs, such as butyric acid and valeric acid, increases as well and inhibits the methanogens further. As the pH continues to decrease, the concentration of undissociated acids inhibits the methanogens additionally. This process failure is subsequently named over-acidification in this article.

In the context of high organic loading rates (OLR), the formation of granules has been shown to increase process stability in anaerobic digesters, which are used in waste water treatment. According to Rajeshwari et al. (2000) the upflow anaerobic sludge blanket (UASB) reactor is operated at a three- to seven-fold higher OLR compared to the continuous stirred tank reactor. A multi-layer model with different substrate gradients offering a habitat for a diverse microbial community was developed to explain the function of granules in the UASB (MacLeod et al. 1990, Guiot et al. 1992, Ahring et al. 1993, Liu et al. 2003, and Satoh et al. 2007). Near the surface of the granules acidogenic bacteria, sulfate-reducing bacteria, and *Methanosarcina* were detected, which tolerate higher VFAs concentrations. In the next inner layer, acetogenic bacteria dominated. In the core of the granules, *Methanosaeta* were mainly found, which only tolerate lower VFAs concentrations.

Another group of bacteria, typically investigated in the context of waste water treatment and enhanced biological phosphorus removal, are the phosphorus-accumulating organisms (PAOs). Thus far, we know from the literature, the ability of PAOs to release phosphate and to take up VFAs under anaerobic conditions and at high concentrations of VFAs (Comeau et al. 1986, Wentzel et al. 1986, Mino et al. 1998, Oehmen et al. 2007). These conditions are fulfilled during the accumulation of organic acids due to process failure. The influence of the PAOs on the biogas formation was not investigated up to now. Under anaerobic conditions, Seviour et al. (2003) and Lemos et al. (2003) observed the formation of poly- $\beta$ -hydroxybutyrate and poly- $\beta$ -hydroxyvalerate with acetic and propionic acid as the substrates, respectively. Polyhydroxyalkanoates can serve as long-term energy storage. Therefore, the PAOs may function as a buffer for VFAs during the over-acidification of the biogas formation process and might play a supporting role in the recovery process.

The aim of this work was to study the mechanism of process recovery and to identify efficient counter measures for the stabilization of the biogas formation process after failure.

## 2. Materials and Methods

### 2.1. Full-scale biogas digester

The full-scale biogas digester was operated at a temperature of approximately 47 °C and its volume was 2300 m<sup>3</sup>. The OLR was around 3.2 kg VS m<sup>-3</sup> d<sup>-1</sup>. The organic substrate consisted of 69 % organic waste (expired foodstuff), 22 % sewage sludge (a mix of primary and secondary sludge from a wastewater treatment plant using “enhanced biological phosphorus removal”), and 9 % grease (contents of fat separators and residues from biodiesel production). The reactor was fed every 4 hours. The hydraulic residence time varied between 18 and 20 days. The sludge in the digester was mixed by a gas lift and pumps. The pumps withdrew sludge at the bottom of the digester and introduced it at either the top or the bottom of the reactor to prevent sedimentation. The outlet pumps for the digested sludge were regulated by the liquid level inside the reactor. For the analyses of the digested sludge, 1 L samples were withdrawn from the outlet of the reactor and from the agitation system. Because this reactor was operated in parallel with another reactor of the same size, the substrate input rates of both reactors were recorded as one parameter, even though the flow rates of each reactor were different. Hence, it was not possible to refer to the exact OLR of each reactor. Thus, the OLR of the full-scale reactor actually refers to the mean value.

### 2.2. Laboratory-scale biogas digesters

The laboratory reactors contained 23 L of sludge (Fig. 1). The temperature was maintained at 50 °C by a thermostat (Thermo Haake B7, Phoenix II) connected to a heating pipe, which was placed around the reactor. The sludge was mixed pneumatically using biogas with a flow of 150 L h<sup>-1</sup> each day for 15 min before the samples were taken and 15 min after the substrate had been introduced. For the biogas recirculation a KNF N86KTE membrane vacuum pump was used.

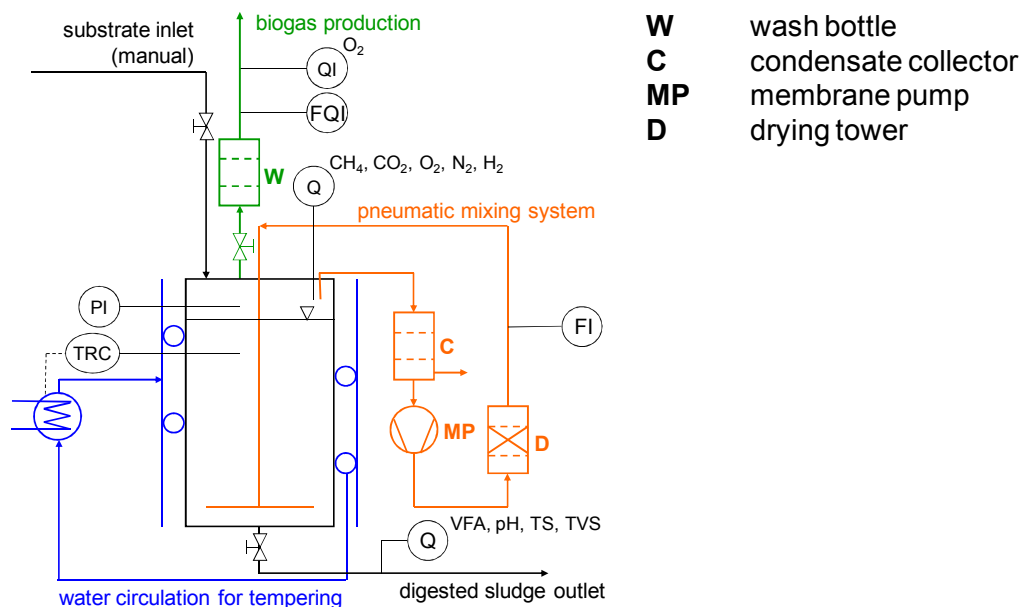


**Figure 1:**

Process scheme for the laboratory digester. Quality (Q, if first letter), quantity (Q, if following letter), indicating (I), flow (F), controlling (C), pressure (P), temperature (T), recording (R).

The substrates were sewage sludge from the investigated full-scale biogas plant and rape oil. The substrates were charged manually every day, after the same amount of digested sludge had been withdrawn before to keep the volume of the reactor content constant. Rape oil was chosen as the co-substrate due to its long chain fatty acids (LCFAs), which are frequently found in real waste water and because its methane yield can be calculated by using the Buswell equation (see also 2.5.). The OLR was dependent on the experimental setup with a base load

between 1.0 and 1.2 kg VS m<sup>-3</sup> d<sup>-1</sup> of sewage sludge. The amount of rape oil was increased up to 9 kg VS m<sup>-3</sup> d<sup>-1</sup> during the experiments to simulate organic overloads. The hydraulic residence time was 20 days. The HRT was calculated by the quotient of the volume of the reactor content divided by the volume of the daily withdrawn digested sludge. During the de-acidification phase rape oil was not added, and sewage sludge was the only substrate fed into the reactor. The OLR was incremented by increasing the amount of rape oil and decreasing the amount of sewage sludge, to keep the flow rate and thus the hydraulic residence time constant. The biogas produced was measured using a Ritter gas meter (TG05/5). For the analyses of the digested sludge, the samples were withdrawn from the outlet of the reactor. The biogas samples were taken from the bypass of the gas pipe between the gas outlet and gas wash bottle, which was placed before the gas meter.

### 2.3. Addition of caustic solutions

The addition of caustic solutions was controlled by adjusting the pH level. When the pH level reached 7.1 or greater the addition was stopped (Tab. 1, Tab. 2, Tab. 3). In the full-scale digester, the amount of NaOH or CaO added were determined by scaling up the amount of NaOH or CaO needed to raise the pH of a withdrawn sample of 500 mL to the pH level of 7.1. This corresponds to the pH at normal operation conditions before process failure.

**Table 1:**

NaOH addition amount per day and loading rate relative to the working volume of the reactor.

Experiment	Time [d]	NaOH addition [mol d <sup>-1</sup> ]	NaOH addition referred to working volume of reactor [mg L <sup>-1</sup> d <sup>-1</sup> ]
Full-scale biogas digester	67	1715	30
	73	5715	99
	74	5715	99
Laboratory-scale NaL	0	0,07	117
	1	0,07	117
	2	0,19	334
	3	0,19	334
	4	0,10	167

**Table 2:**

Measured calcium concentration compared to the expected calcium concentration elevation due to the addition of CaO.

Experiment	time [d]	CaO addition [mol d <sup>-1</sup> ]	Expected elevation of calcium conc. [mg L <sup>-1</sup> ]	Measured calcium conc. on the next day [mg L <sup>-1</sup> ]
Full-scale biogas digester	79	10 699	261	< 5
	80	10 699	261	6
	86	5 350	130	17
	87	5 350	130	20
Laboratory-scale CaL	0	0.09	219	22
	1	0.09	219	18
	2	0.09	219	10
	3	0.09	219	< 5
	4	0.18	439	< 5
	5	0.18	439	< 5
	6	0.36	877	< 5
7	0.36	877	9	

In the laboratory-scale reactors, the amount of NaOH and CaO corresponds to the scaled down amount used within the first days in the full-scale process recovery. However, due to different levels of over-acidification, the amount of additives had to be adapted to the VFAs concentration. The caustic solutions were added as an “impact load” - one time a day.

**Table 3:**

Comparison between the effect of NaOH and CaO on the concentration of VFAs each day and the resulting pH on the next day. Because the pH was measured several times a day at the full-scale biogas plant, the last pH value before the next charge is listed.

Experiment	NaOH			CaO		
	Time [d]	NaOH addition [mol L <sup>-1</sup> d <sup>-1</sup> ]/ VFA [mol L <sup>-1</sup> ]	pH next day after NaOH addition	Time [d]	CaO addition [mol L <sup>-1</sup> d <sup>-1</sup> ]/ VFA [mol L <sup>-1</sup> ]	pH next day after CaO addition
Full-scale biogas digester	67	0.02	6.85	78	0.10	6.87
	73	0.07	7.03	79	0.09	6.89
	74	0.06	7.08	85	0.04	6.97
				86	0.04	7.05
Laboratory-scale NaL & CaL	0	0.03	6.70	0	0.03	5.67
	1	0.03	6.76	1	0.03	5.63
	2	0.08	6.95	2	0.03	5.63
	3	0.08	7.00	3	0.03	5.75
	4	0.04	7.74	4	0.06	6.49
				5	0.06	6.56
				6	0.13	6.85
7				0.15	7.25	

#### 2.4. Chemical, gas, and SEM analyses

The temperature and pH were measured in the digested sludge samples by a WTW pH 340i using a Sen Tix 41 pH electrode.

For the total solids (TS) and the volatile solids (VS), the samples were dried at 105 °C in a Memmert drying chamber for 24 h and then burned at 550 °C (Nabertherm Controller B170). The weight of the samples was determined using a Sartorius CP220S-OCE weighing machine (scale +/- 0.01 g). The TS and VS were analyzed according to the German guideline DIN 38409-1.

Total volatile fatty acids (VFAs) (LCK 365), phosphate (LCK 350), and calcium (LCK 327) concentrations were determined photometrically (Hach-Lange DR2800) after the samples had been centrifuged twice at 10,000 rpm for 10 min (Eppendorf Centrifuge 5804). Although the detection limit for the calcium concentration was at 5 mg L<sup>-1</sup>, values measured below 5 mg L<sup>-1</sup> were included in the graphs 3c and 3f, in order to show the low concentration of calcium.

The individual short chain fatty acids (C<sub>2</sub>H<sub>4</sub>O<sub>2</sub> to C<sub>5</sub>H<sub>10</sub>O<sub>2</sub>) were determined by ion chromatography (IC) (DIONEX ICS 3000, CA, USA). The eluent was sodium hydroxide and the IC was equipped with an AS11-HC column. The carbon value of the C/P-ratio was calculated using the carbon content of the individual short chain fatty acids.

The gas composition was determined by gas chromatography (SRI 8610C; SRI Instruments, Torrance, USA). The gas chromatograph was equipped with a thermal conductivity detector, a 6' x 1/8" S.S. silica gel packed column and a 6' x 1/8" S.S. molecular sieve 13X packed column (SRI Instruments, USA). Argon was used as the carrier gas. The analyzed gas components were hydrogen, oxygen, nitrogen, methane, and carbon dioxide.

The aggregates and their fragments were analyzed using a Scanning Electron Microscope (SEM) Ultra 55 Plus (Carl Zeiss SMT) with an energy dispersive spectrometer (EDS) in order to determine chemical composition and to characterize their microstructure and morphology. Analyzed images were taken using a secondary electron

detector (SE2). Analyses were performed at 20 kV accelerating voltage. Chemical identification of elements in spectra was possible using a NSS analytical system. All samples studied with SEM were carbon coated. The p-cresols (4-methylphenol) were analyzed qualitatively by a commercial laboratory using gas chromatography - mass spectrometry - screening.

### 2.5. Determination of the expected methane yields in the laboratory experiments

The expected value for the methane yield of sewage sludge was determined using results gained during a stable process at a very low OLR at  $2.5 \text{ kg VS m}^{-3} \text{ d}^{-1}$ . For the expected methane yield of rape oil, the Buswell equation was used according to Buswell et al. (1952).

## 3. Results

### 3.1. Process failure and recovery in a full-scale biogas reactor

Process failure occurred after several years of a stable biogas process operation in a full-scale reactor. According to the operator, the failure was caused by p-cresols that were accidentally introduced with the sewage sludge. The process failure was evidenced by a factor of five decrease in the production of biogas and a corresponding factor of ten increase in the concentration of VFAs (Fig. 2).

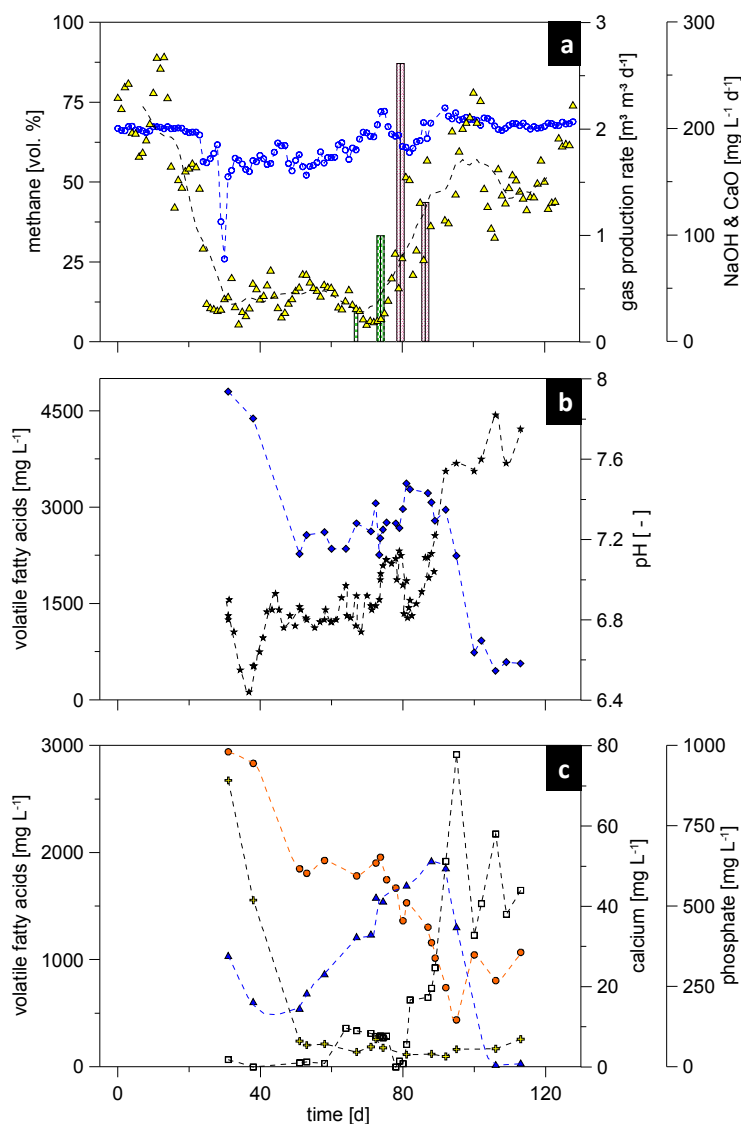


**Figure 2:**

Full-scale reactor: (a) Methane content in the biogas  $\circ$  and gas production rate  $\triangle$  during process failure and recovery in the presence of NaOH  $\square$  and CaO  $\square$  (added amount of caustic solution with respect to the sludge volume in the digester). (b) Concentration of volatile fatty acids (VFAs)  $\diamond$  and pH  $\star$  (c) Concentration of acetic acid  $\square$ , propionic acid  $\triangle$ , phosphate  $\circ$ , and calcium  $\square$

In a first counter measure, the OLR was reduced from  $3.2 \text{ kg VS m}^{-3} \text{ d}^{-1}$  to approximately 50 % of that value on day 24. One week later, the OLR was further diminished by 50 % for one week. At that time, the methane content was between 26 and 57 vol. %, and the pH ranged between 6.4 and 6.9. To accelerate the stabilization of biogas production, NaOH was added to increase the pH (Fig. 2b). After the addition of NaOH (Tab. 1), the pH was above 7.0 for one week, but once again decreased below pH 7.0 after the increase of the OLR, and the propionic acid concentration increased further from  $1,210$  to  $1,590 \text{ mg L}^{-1}$  (Fig. 2c). In a third counter measure, CaO was introduced. Five days after the last addition of CaO, the concentration of propionic acid decreased rapidly. During this time, the calcium concentration reached its maximum level of  $80 \text{ mg L}^{-1}$ . Although the first two CaO dosages were nearly double the size of the later ones, the calcium concentration increased significantly after the later dosages. The calcium concentration in the liquid phase was up to 60 times lower than expected considering the concentration of CaO added (Tab. 2). After the first CaO addition, the gas production rate increased until the addition one week later by a factor of three and the methane content increased from 64 to 68 vol. % (Fig. 2a). One week after the last CaO addition the gas production rate reached its expected level and the methane yield was at 70 vol. %.

Before calcium oxide was added, the trend of the phosphate concentration was similar to that of VFAs concentration (Fig. 2c). After the addition of CaO, the phosphate concentration exhibited a reverse trend to what was observed for calcium. When the phosphate concentration increased, the calcium concentration decreased and vice versa. When the concentration of VFAs was low, the phosphate concentration only accounted for 30 % of the concentration at the beginning of the process failure.

### 3.2. Process failure at laboratory-scale biogas reactors

To achieve a deeper understanding of the effects of additives on the enhancement of process stability, two experiments were performed. In both experiments, process failure was provoked by the addition of excess organic matter. Therefore the amount of rape oil was increased, thus the OLR was a factor 3.3 higher at  $10 \text{ kg VS m}^{-3} \text{ d}^{-1}$ . As soon as the methane yield decreased by more than 90 % and the VFAs concentrations rose more than 10 times ( $> 6,000 \text{ mg L}^{-1}$ ), the OLR was reduced by a factor of nine and either NaOH or CaO were added.

#### 3.2.1. Experiment NaL: process recovery using NaOH

The amount of NaOH dosage implemented in the first two days was of the same magnitude as the amount added to the full-scale reactor, adjusted to the reactor volume (Tab. 1). Because neither the VFAs concentration nor the gas production rate ( $0.2 \text{ L h}^{-1}$ ) changed, the amount of NaOH added was further increased until the pH rose to above 7.0 on day 5 (Fig. 3a-c). After the last NaOH addition, almost one week had passed until the sum of VFAs decreased below  $1,000 \text{ mg L}^{-1}$ , while the methane yield increased to  $1 \text{ m}^3 (\text{kg VS})^{-1}$  (Fig. 3c).

Before the first NaOH addition, the LCFAs dominated in the composition of VFAs at approximately 63 %. The LCFAs did not decrease until day 10 (Fig. 3a). In the beginning, the concentration of acetic acid was  $1100 \text{ mg L}^{-1}$  and that of propionic acid was  $800 \text{ mg L}^{-1}$ . On day 18, propionic acid concentration decreased to less than  $100 \text{ mg L}^{-1}$ . At this point, the calcium concentration reached its maximum (Fig. 3c). After the re-start of co-digestion of sewage sludge and oil on day 22 (Fig. 3a), the VFAs increased to almost the same level as it was at the beginning of the process recovery. The methane production rate decreased correspondingly.

The course of the phosphate concentration was similar to that of VFAs, particularly that of acetic and propionic acids (Fig. 3b). However, the calcium concentration exhibited an opposite trend (Fig. 3c). At high phosphate concentrations ( $1,000 \text{ mg L}^{-1}$ ), the calcium concentration was low ( $10 \text{ mg L}^{-1}$  and below) and vice versa ( $\text{PO}_4^{3-}$ :  $300 \text{ mg L}^{-1}$ ;  $\text{Ca}^{2+}$ :  $50 \text{ mg L}^{-1}$ ). It should be noted that the concentration of propionic and acetic acids rapidly decreased as soon as the calcium concentration reached its maximum, even though the hydrogen partial pressure (approximately 0.16 mbar, data not shown) was almost two-fold higher than the limit of the thermodynamic window for degradation of propionic acid.



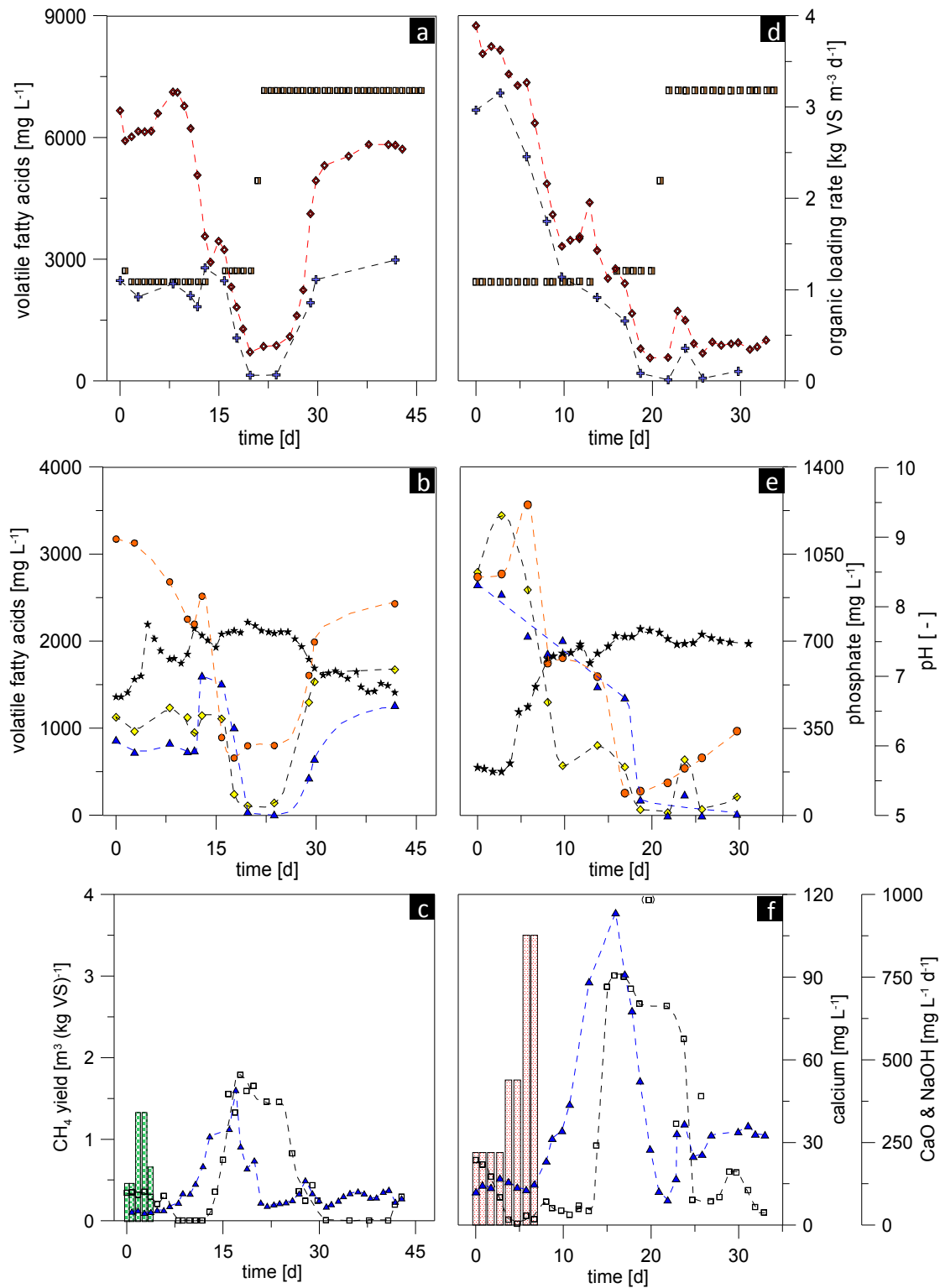


**Figure 3:**

(a) NaL, (d) CaL: The concentration of VFAs  $\blacklozenge$  (analyzed using Hach-Lange) and the sum of short chain fatty acids ( $C_2H_4O_2$  to  $C_5H_{10}O_2$ )  $\blacksquare$  (analyzed using IC) during process recovery and the increase of the OLR  $\blacksquare$  starting on day 22. LCFAs can be estimated from the difference between the concentrations of the sum of VFAs and the sum of short chain fatty acids. (b) NaL, (e) CaL: Concentration of acetic acid  $\blacklozenge$ , propionic acid  $\blacktriangle$ , phosphate  $\bullet$ , and the pH  $\star$  during process recovery (c) NaL, (f) CaL: Concentration of phosphate  $\bullet$ , calcium  $\square$ , and methane yield  $\blacktriangle$  during process recovery with NaOH  $\blacksquare$  or CaO  $\blacksquare$  (added amount of caustic solution with respect to the sludge volume in the digester).

### 3.2.2. Experiment CaL: process recovery using CaO

After four days of CaO additions (Tab. 2), neither the pH (Fig. 3e-f) nor the gas production rate increased. Therefore, the concentration of CaO added was further increased until the pH reached a value of greater than 7.0. However, the VFAs concentration had begun to decrease after the first addition of CaO (Fig. 3d), and the calcium concentration remained below the expected value (Tab. 2).

The biogas production rate started to increase after the last CaO dosage. Within five days it multiplied almost eight times its initial value, although the VFAs content was still  $3,000 \text{ mg L}^{-1}$ . At this time, the methane yield was seven times higher than the expected value from the OLR of  $1.2 \text{ kg m}^{-3} \text{ d}^{-1}$ . On day 20, the substrate accumulation in the reactor was degraded and the concentration of VFAs was low. The re-start of co-substrate dosage was followed by a temporary decrease in the biogas production and an increase in the VFAs content. However after five days, the concentration of VFAs decreased again below  $1,000 \text{ mg L}^{-1}$ , and the methane yield and gas production rate were in the expected range.

During process failure, the VFAs consisted mainly of acetic and propionic acid. LCFAs comprised only 12 % of the total VFAs (Fig. 3d). Within the first six days, the concentration of acetic acid was higher than that of propionic acid (Fig. 3e). The acetic acid concentration first increased slightly to  $3,500 \text{ mg L}^{-1}$ , but then decreased to  $500 \text{ mg L}^{-1}$  within one week. The propionic acid decreased from  $2,660$  to  $1,360 \text{ mg L}^{-1}$  within the first 17 days. One day later, the concentration had decreased to  $180 \text{ mg L}^{-1}$ . At this time, the calcium concentration reached its maximum. After the re-start of the co-substrate dosage, a small amount of acetic ( $640 \text{ mg L}^{-1}$ ) and propionic acid ( $240 \text{ mg L}^{-1}$ ) accumulated, but within two days, the concentrations decreased to the level observed on day 22.

The concentration dependence of phosphate was similar to that of VFAs (Fig. 3e). High acid concentrations correlated with a high phosphate concentration (approximately  $1,250 \text{ mg L}^{-1}$ ) and low acid concentrations with a low phosphate concentration (approximately  $90 \text{ mg L}^{-1}$ ). The course of calcium concentration exhibited an opposite trend relative to the phosphate and VFAs concentrations (Fig. 3f). The calcium concentration in the liquid phase decreased from  $28 \text{ mg L}^{-1}$  to less than  $5 \text{ mg L}^{-1}$  on day 8, even though calcium oxide was added, while the phosphate concentration increased slightly to its maximum. When the calcium concentration increased and reached its maximum level at approximately  $90 \text{ mg L}^{-1}$ , the phosphate concentration decreased to its minimum.

The partial pressure of hydrogen was at 0.1 mbar and greater, and thus exceeded two-to three-times the limit of the thermodynamic window for the degradation of propionic acid until day 17. However, propionic acid decreased at a rate of  $3.3 \text{ mg L}^{-1} \text{ h}^{-1}$ . After day 17, the hydrogen partial pressure was within the thermodynamic window, and the rate of propionic acid decrease was enhanced by a factor of nine.

### 3.3. Digested sludge structure

While no change in the structure of digested sludge was observed during the experiment NaL, small white particles were found in the digested sludge after the introduction of CaO. The addition of sulfuric acid to the particles did not result in a release of carbon dioxide, indicating that these particles were not calcium carbonate.

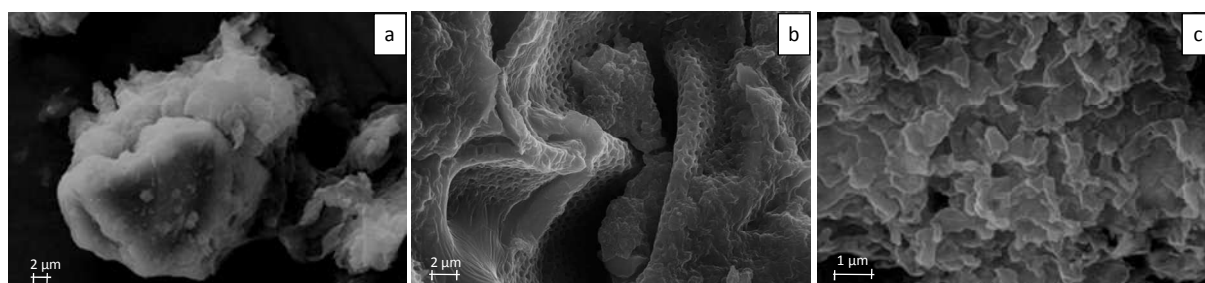


**Figure 4:**

SEM (SE2-Detector): (a) Inner part of a big aggregate (7cm) found in experiment CaL: silicate mineral covered by aggregates composed of calcium rich phosphate minerals (b) Inner part of a big aggregate (7 cm) found in experiment CaL: composed of a mixture of phosphate minerals characterized by porous structures (c) Surface of a small aggregate (2mm) from a very similar experiment as CaL: consisting of mainly carbon and calcium.

Besides the small particles (0,5 - 5 mm), big aggregates with a diameter of up to 7 cm were found in experiment CaL, when the reactor was opened on day 12. Macroscopically, the big aggregate exhibited a layered structure. It consisted of a dark core part surrounded by light in color outer parts. Scanning electron microscopy images showed chaotic texture of the aggregates. SEM-EDS analyses demonstrated high concentrations of carbon on the surface and high concentrations of phosphate and calcium in the core of the aggregates (Fig. 4). All phases exhibited xenomorphic shapes.

#### 4. Discussion

CaO additions into the biogas digester were more successful than NaOH additions to stabilize the process of biogas formation. When the OLR was increased, organic acids accumulated again in the laboratory-scale reactor treated with NaOH, thus the process recovery with NaOH was not sustainable. However, the process recovery with CaO was sustainable indicated by a stable process after the increase of the OLR. Hence, the results of the laboratory experiments supported the interpretation of the observations in the full-scale biogas plant during the process recovery: In the full-scale biogas digester, the NaOH addition did not stabilize the process of biogas formation, even though the pH was above 7.0 for one week after the last NaOH addition. The propionic acid concentration increased further and with an increasing OLR, the pH decreased again below 7.0 indicating the continuation of the process failure. In contrast, after the first two days of CaO addition, the acid content decreased slightly, even though the pH was still below 7.0. As soon as the pH reached 7.1 due to further addition of CaO, the VFAs concentration decreased rapidly, and the process of biogas formation became stable, even though the OLR was increased again. In the laboratory experiment NaL, the VFAs content started to decrease after the pH was raised above 7.0 for one week; in contrast, during the in experiment CaL, the VFAs concentrations already decreased when the pH was still below 7.0. In this context, the calcium concentration seemed to play an important role. As soon as the calcium concentration increased in NaL and as soon as CaO was added in CaL, acids concentrations decreased. The investigations of the process recovery in the full-scale biogas digester also showed a rapid decrease in VFAs content after the calcium concentration increased significantly.

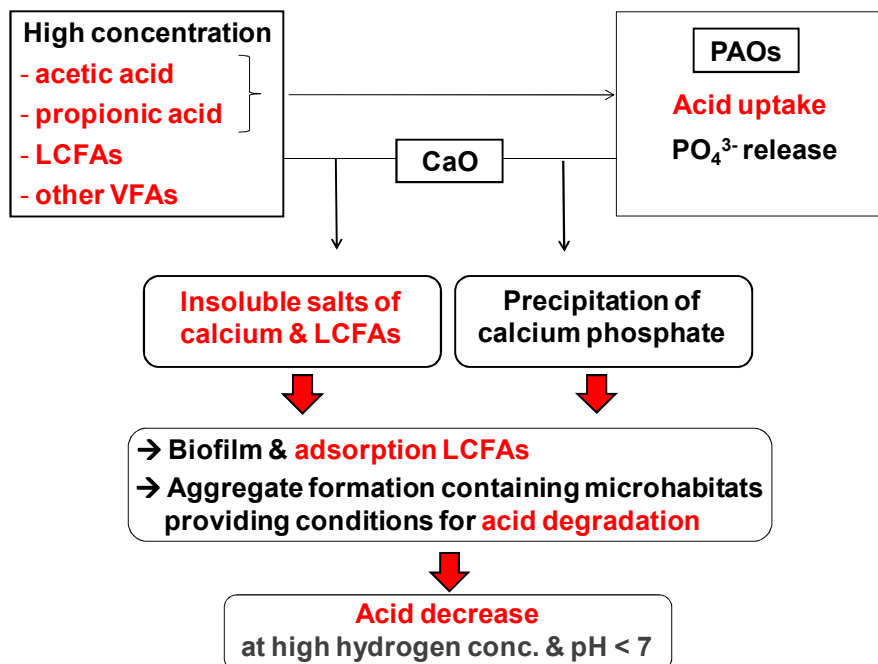


**Figure 5:**

Mechanism of process recovery via the addition of CaO; LCFAs (long chain fatty acids); CaO (calcium oxide); and PAOs (phosphorus-accumulating organisms).

This phenomenon and the observation of small white particles in correlation with CaO additions lead to the hypothesis that the decrease in acid content was dependent on different processes, including:

- formation of insoluble calcium salts with LCFAs and phosphate
- adsorption of acids on calcium precipitates resulting in the formation of aggregates
- the activity of PAOs taking up VFAs and releasing phosphates
- the creation of microhabitats within the aggregates providing favorable conditions for the microbial degradation of VFAs and hydrogen

These processes (Fig. 5) will be discussed in more detail.

#### *4.1. Precipitation of calcium salts with LCFAs and adsorption of acids*

The formation of aggregates was observed in the digested sludge of CaL and the full-scale biogas digester after the addition of CaO. Scanning electron microscopy analyses revealed calcium phosphate compounds in the core of the aggregates and carbon rich matter on the surface of the aggregates. The carbon was derived most likely from the LCFAs, which led to lower LCFAs concentrations in the liquid phase of CaL relative to NaL. Thus, the addition of CaO resulted in the formation of insoluble salts of calcium with LCFAs. Rinzema et al. (1993) and Hwu et al. (1998) also observed the adsorption of LCFAs salts accumulating on granules in a solid-like layer and in the pore space of aggregates, which were formed by small pellets of a UASB reactor.

Additionally, in all own experiments the measured calcium concentrations in the liquid phase were significantly below the expected concentration after the addition of CaO (Tab. 2). This indicates precipitation processes. The reduction of LCFAs in the liquid phase by precipitation and adsorption enabled a reversal of process inhibition. Even though the aggregate formation played a minor role in the de-acidification process in NaL, it is assumed that some calcium LCFAs salts were formed from calcium that originated from the charged sewage sludge, because the calcium concentration decreased. After re-activation of biogas production, the high methane yield indicated the degradation of VFAs and LCFAs retained in the reactor during the over-acidification phase. Consequently, an increase in calcium content was observed (Fig. 3f). After the increase of the OLR, the amount of calcium available to precipitate LCFAs and to create aggregates was obviously not sufficient to buffer the increase of acids resulting from the re-start of co-substrate charging. Hence, a process failure occurred again. Because the precipitation of LCFAs and the formation of aggregates played a major role in CaL, significantly more organic matter was retained in the reactor by aggregate formation, and therefore the methane yield during the process recovery was seven times higher than expected relative to the current OLR. During process recovery, the increase of calcium concentration indicated clearly the degradation of LCFA which had been precipitated with calcium before. The small increase in the acid content after the re-start of co-digestion was probably buffered due to the higher availability of dissolved calcium in the sludge. The precipitation and adsorption of acids by calcium and aggregates served as a buffer between the production of acids from fermentation and the degradation of acids by methanogens. Hence, the process recovery with CaO was sustainable.

#### *4.2. Precipitation of calcium phosphate*

During the over-acidification in experiment NaL, the calcium concentration decreased with increasing phosphate concentration. In experiment CaL and in the full-scale reactor, phosphate concentration quickly decreased, when the availability of calcium increased due to CaO additions. These observations indicate the precipitation of calcium phosphate. Scanning electron microscopy analyses revealed the presence of calcium phosphate in the core of the aggregates. However, these analyses could not determine the mineral phases of the aggregates.

Taking into account that local heterogeneities are favored during aggregate formation, it seems very likely that calcium phosphate was formed after CaO was added. Furthermore, calcium is known to be involved in biologically induced creation of granules (Aivasidis et al. 2005). Frankel et al. (2003) showed that the rate of mineralization can become several orders of magnitude faster than inorganic mineralization, if microorganisms are involved.

#### 4.3. Activity of phosphorus-accumulating organisms (PAOs)

During the accumulation of VFAs, the phosphate concentration increased correspondingly to the increase in the VFAs concentration. However, there was no extra phosphate source added to the substrate, thus the phosphate originated from either precipitates, which became soluble, or PAOs, which released phosphate under the specific conditions. Because the calcium concentration did not increase, no calcium phosphate precipitates became soluble. However, the milieu was anaerobic and contained a sufficient amount of VFAs, which were generated during the process failure. Thus the conditions for the PAOs were satisfied, allowing for the release of phosphate and promoting the uptake of acids. In particular, when propionic and acetic acid were found in high concentrations, the concentration of phosphate was high as well and vice versa. As shown by Liu et al. (1996), the PAOs are active at a pH below 7.0. The optimal pH for the uptake of acetic acid is 6.8. This might be one reason for the decrease in the concentration of acetic and propionic acids in the experiment CaL, when the pH was still below 7.0. According to Röske et al. (2005), the PAOs need a seven- to ten-fold excess of easily degradable organic matter with respect to the total phosphorous concentration. Therefore, the PAOs released phosphate during the accumulation of VFAs. In the experiment CaL, the ratio between the carbon of short chain fatty acids and the phosphorous content (C/P) ranged between 7 and 30 until day 17. Thus, the PAOs likely contributed to the decrease of VFAs content by taking up acids and releasing phosphate in the experiment CaL, when the pH was below 7.0 in the first five days. Due to the precipitation of calcium phosphate compounds, this phosphate release could not be observed in the liquid phase as an increase in the phosphate concentration.

The hypothesis regarding the involvement of the PAOs is supported by the results of molecular biological analyses of the microbial community from experiments performed using the same substrates and inoculum from the same source. The results of Lerm et al. 2011 indicate that *Actinobacteria* became more dominant during the over-acidification process. *Actinobacteria* are frequently found in plants using enhanced biological phosphorus removal (Seviour et al. 2008).

Lemos et al. (2003) showed that first propionic acid, then butyric acid, and later on acetic acid were taken up by the PAOs. This succession of uptake was not observed in this work. Butyric acid concentration usually decreased at the same time as that of acetic acid or even earlier. The propionic acid tended to decrease after the acetic acid. This is consistent with the results of Pijuan et al. (2004), who observed that the uptake of acetic acid occurred prior to that of the propionic acid. Consequently, phosphate release had taken place faster due to the acetic acid rather than the propionic acid. This might have contributed to a decrease in the acetic acid concentration at a higher rate than that of propionic acid in an acidic milieu.

#### 4.4. Processes within the aggregates and the influence of biofilm on the degradation of aggregates

The presence of calcium and phosphate in the core of the aggregates indicates that calcium and phosphate concentrations exceeded locally the liquid solubility of calcium phosphate compounds. While the calcium originated from the CaO additions, the availability of phosphate was dependent on the activity of PAOs as discussed in 4.3. When the PAOs released phosphate, they took up VFAs and thereby decreased the acid concentration in the aggregates. The local decrease in VFAs concentration probably allowed the hydrogenotrophic microorganisms to consume much of the hydrogen in the aggregates, which was produced by fermentative bacteria. This in consequence, enabled acetogenic bacteria to degrade the propionic acid in the aggregates, even though the hydrogen concentration in the gaseous phase was two- to three times too high allowing for degradation. According to Harper et al. (1986), the hydrogen partial pressure has to be below 0.1 mbar that the degradation of propionic acid can take place. In agreement, Fukuzaki et al. (1990) also observed the degradation of propionic acid, although the hydrogen partial pressure in the gaseous phase was too high. They concluded that bacteria inside of floc structures seem to be protected from the hydrogen partial pressure outside the flocs.

In another laboratory experiment under similar process conditions (data not shown, Kleyböcker et al., in prep.) a big aggregate with a diameter of 5 cm was observed. In the inner part of the aggregate, the pH was neutral, while the pH became more acidic in the outer layers. It is assumed that the structure of the big aggregate is similar to that of the aggregates observed in the presented experiments. Thus, the processes in the aggregates are very likely similar to the ones described by MacLeod et al. (1990) for granules in UASB reactors.

The aggregates in the CaL experiment disappeared quickly after the process of biogas formation had become stable for several days. This indicates that LCFAs were degraded by microorganisms growing as a biofilm on and within the aggregates. Similar observations are reported for granules in the literature (van Langerak et al. 1998, Hwu et al. 1998, and Chipasa et al. 2006).

## 5. Summary and Conclusions

The mechanism of the process recovery by the addition of CaO was found to be dependent on the formation of aggregates containing insoluble salts of calcium and LCFAs as well as calcium phosphate and on the adsorption of acids on the surface of the aggregates. It is very likely that PAOs were involved in the aggregate formation by releasing phosphate during uptake of short chain fatty acids. Precipitation of calcium phosphates served as the core upon which insoluble salts of calcium and LCFAs were adsorbed together with VFAs promoting the growth of microbial biofilms. These processes resulted in aggregate formation that provided different microhabitats wherein the concentration of short chain fatty acids were initially lowered by the uptake of PAO and later on by the activity of methanogens. The hydrogen concentration in the aggregates was lower than in the gas phase due to a continuous consumption by methanogens that allowed for the degradation of propionic acid. Additionally, the PAOs contributed to a decrease in the VFAs by taking up acids.

In summary, the addition of CaO as a counter measure to increase the pH during process failure is highly recommended, because the availability of calcium also enables aggregate formation and has thereby additionally a stabilizing effect on the process of biogas formation. Another advantage of this counter measure is that aggregates dissolve after the process is stabilized, and the retained fatty acids can be later converted into biogas. The addition of NaOH is not recommended, as significantly much more time is required to stabilize the process, even though the pH reaches its neutral value earlier than in the case of CaO.

## Acknowledgments

Thanks to Andrea Vieth-Hillebrand and her team, Section for Organic Geochemistry at GFZ, for analyzing short chain fatty acids by ion chromatography. Personal thanks to Rona Miethling-Graff, Stephanie Lerm, Tobias Lienen and, Daria Morozova for helpful suggestions.

The results presented in this paper were gained during the “Co-fermentation” project financed by the Volkswagen Foundation (II/80 703) and during the “Optgas” project (03KB018A) funded by the Federal Ministry for the Environment, Nature Conservation and Nuclear Safety.

## List of abbreviations

CaL	experiment in a laboratory-scale reactor using CaO for de-acidification
CaO	calcium oxide
IC	ion chromatography
LCFAs	long chain fatty acids
NaL	experiment in a laboratory-scale reactor using NaOH for de-acidification
NaOH	sodium hydroxide
OLR	organic loading rate
PAOs	phosphorus-accumulating organisms
SEM	scanning electron microscope
TS	total solids
VFAs	volatile fatty acids
VS	volatile solids

## References

- Ahring, B., Schmidt, J., Winther-Nielsen, M., Macario, A., Conway de Marcario, E., 1993. Effect of medium composition and sludge removal on the production, composition, and architecture of thermophilic (55°C) acetate-utilizing granules from an upflow anaerobic sludge blanket reactor, *Applied and Environmental Microbiology* 59, 8, 2538-2545.
- Aivasidis, A., Diamantis, V., 2005. Biochemical reaction engineering and process development in anaerobic wastewater treatment, *Advances in Biochemical Engineering/Biotechnology* 92, 49-76.
- Angelidaki, I., Ahring, B., 1992. Effects of free long-chain fatty acids on thermophilic anaerobic digestion, *Applied Microbiology and Biotechnology* 37, 808-812.
- Balussou, D., Kleyböcker, A., McKenna, R., Möst, D., Fichtner, W., 2012. An economic analysis of three operational co-digestion biogas plants in Germany, *Waste and Biomass Valorization*, 3, 1, 23-41.
- Braun, R., Huber, P., Meyrath, J., 1981. Ammonia toxicity in liquid piggery manure digestion, *Biotechnology Letters* 3, 4, 159-164.
- Buswell, A., Müller, H., 1952. Mechanism of methane fermentation, *Industrial and Engineering Chemistry*, 44, 3, 550-552.
- Chipasa, K., Medrzycka, K., 2006. Behaviour of lipids in biological wastewater treatment processes, *Journal of Industrial Microbiology and Biotechnology* 33, 635-645.
- Comeau, Y., Hall, K., Hancock, R., Oldham, W., 1986. Biochemical model for enhanced biological phosphorus removal, *Water Research* 20, 12, 1511-1521.
- Frankel, R., Bazylnski, D., 2003. Biologically induced mineralization by bacteria, *Reviews in Mineralogy and Geochemistry* 54, 1, 95-114.
- Fukuzaki, S., Nishio, N., Shobayashi, M., Nagai, S., 1989. Inhibition of the fermentation of propionate to methane by hydrogen, acetate, and propionate, *Applied and Environmental Microbiology* 56, 3, 719-723.
- Guiot, S., Paus, A., 1992. A structured model of the anaerobic granule consortium, *Water, Science and Technology* 25, 7, 1-10.
- Harper, S., Pohland, F., 1986. Recent developments in hydrogen management during anaerobic biological wastewater treatment, *Biotechnology and Bioengineering* 28, 585-602.
- Hwu, C., Tseng, S., Yuan, C., Kulik, Z., Letting, G., 1998. Biosorption of long-chain fatty acids in USAB treatment process, *Water Research* 32, 5, 1571-1579.
- Karakashev, D., Batstone, D., Angelidaki, I., 2005. Influence of environmental conditions on methanogenic compositions in anaerobic biogas reactors, *Applied and Environmental Microbiology* 71, 1, 331-338.
- Kleyböcker, A., Liebrich, M., Seyfarth, D., Kraume, M., Würdemann, H., (in prep.). Early warning indicator (EWI) in terms of over-acidification.
- Kuang, Y., Pullammanappallil, P., Lepesteur, M., Ho, G., 2006. Recovery of oleate-inhibited anaerobic digestion by addition of simple substrates, *Journal of Chemical Technology and Biotechnology* 81, 1057-1063.
- Lemos, P., Serafim, L., Santos, M., Reis, M., Santos H., 2003. Metabolic pathway for propionate utilization by phosphorus-accumulating organisms in activated sludge: <sup>13</sup>C labeling and in vivo nuclear magnetic resonance, *Applied and Environmental Microbiology* 69, 1, 241-251.
- Lerm, S., Kleyböcker, A., Miethling-Graff, R., Vieth-Hillbrand, A., Alawi, M., Kasina, M., Liebrich, M., Würdemann, H., 2012. Archaeal community composition affects the function of anaerobic co-digesters in response to organic overloads, *Waste Management*, 32, 3, 389-399.
- Liu, W., Mino, T., Matsuo, T., Nakamura, K., 1996. Biological phosphorus removal process – effect of pH on anaerobic substrate metabolism, *Water Science and Technology* 34, 1-2, 25-32.
- Liu, Y., Xu, H., Yang, S., Tay, J., 2003. Mechanisms and models for anaerobic granulation in upflow anaerobic sludge blanket reactor, *Water Research* 37, 661-673.
- Luostarinen, S., Luste, S., Sillanpää, M., 2009. Increased biogas production at wastewater treatment plants through co-digestion of sewage sludge with grease trap sludge from meat processing plant, *Bioresource Technology* 100, 79-85.
- MacLeod, F., Guiot, S., Costerton, J., 1990. Layered structure of bacterial aggregates produced in an upflow anaerobic sludge bed and filter reactor, *Applied and Environmental Microbiology* 56, 6, 1598-1607.
- Mino, T., van Loosdrecht, M., Heijnen, J., 1998. Microbiology and biochemistry of the enhanced biological phosphate removal process, *Water Research* 32, 11, 3193-3207.

- Miron, Y., Zeeman, G., van Lier, J., Letting, G., 2000. The role of sludge retention time in the hydrolysis and acidification of lipids, carbohydrates and proteins during digestion of primary sludge in CSTR systems, *Water Research* 34, 5, 1705-1713.
- Oehmen, A., Lemos, P., Carvalho, G., Yuan, Z., Keller, J., Blackall, L., Reis, M., 2007. Advances in enhanced biological phosphorus removal: From micro to macro scale, *Water Research* 41, 2271-2300.
- Pender, S., Toomey, M., Carton, M., Eardly, D., Patching, J., Colleran, E., O'Flaherty, V., 2004. Long-term effects of operating temperature and sulphate addition on the methanogenic community structure of anaerobic hybrid reactors, *Water Research* 38, 619-630.
- Pijuan, M., Saunders, A., Guisasola, A., Baeza, J., Casas, C., Blackall, L., 2004. Enhanced biological phosphorus removal in a sequencing batch reactor using propionate as a sole carbon source, *Biotechnology and Bioengineering* 85, 1, 56-67.
- Rajeshwari, K., Balakrishnan, M., Kansal, A., Lata, K., Kishore, V., 2000. State-of-the-art of anaerobic digestion technology for industrial wastewater treatment, *Renewable and Sustainable Energy Reviews* 4, 135-156.
- Rinzema, A., Alphenaar, A., Lettinga, G., 1993. Anaerobic digestion of long-chain fatty acids in UASB and expanded granular sludge bed reactors, *Process Biochemistry* 28, 527-537.
- Röske, I., Uhlmann, D., 2005. *Biologie der Wasser und Abwasserbehandlung*, Verlag Eugen Ulmer Stuttgart.
- Satoh, H., Miura, Y., Tsushima, I., Okabe, S., 2007. Layered structure of bacterial and archaeal communities and their in situ activities in anaerobic granules, *Applied and Environmental Microbiology* 73, 22, 7300-7307.
- Schink, B., 1997. Energetics of syntrophic cooperation in methanogenic degradation, *Microbiology and Molecular Biology Reviews* 61, 2, 262-280.
- Seviour, R., Kragelund, C., Kong, Y., Eales, K., Nielsen, J., Nielsen, P., 2008. Ecophysiology of the *Actinobacteria* in activated sludge systems, *Antonie van Leeuwenhoek* 94, 21-33.
- Seviour, R., Mino, T., Onuki, M., 2003. The microbiology of biological phosphorus removal in activated sludge systems, *FEMS Microbiology Reviews* 27, 99-127.
- van Langerak, E., Gonzalez-Gil, G., van Aelst, A., van Lier, J., Hamelers, H., Lettinga, G., 1998. Effects of high calcium concentrations on the development of methanogenic sludge in upflow anaerobic sludge bed (UASB) reactors, *Water Research* 32, 4, 1255-1263.
- Veeresh, G., Kumar, P., Mehrotra, I., 2005. Treatment of phenol and cresols in upflow anaerobic sludge blanket (UASB) process: a review, *Water Research*, 39, 154-170.
- Wentzel, M., Lötter, L., Loewenthal, R., Marais, G., 1986. Metabolic behaviour of *Acinetobacter* spp. In enhanced biological phosphorus removal – a biochemical model, *Water SA* 12, 4, 209-224.